

### Science and Technology of Welding and Joining



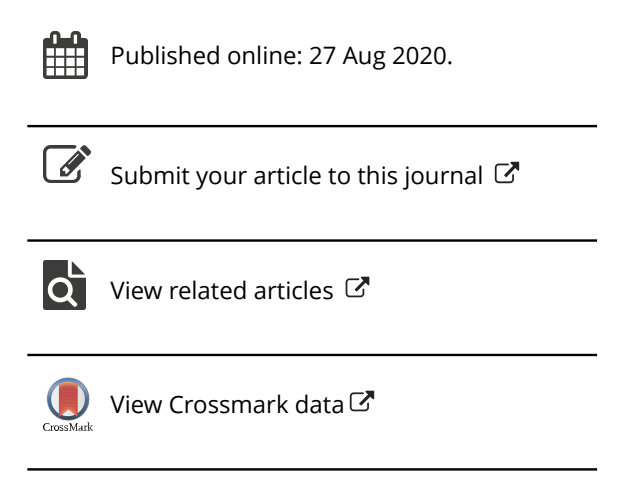
ISSN: (Print) (Online) Journal homepage: https://www.tandfonline.com/loi/ystw20

# Evaluating susceptibility of carbon steels to solidification cracking by transverse-motion weldability test

Chunzhi Xia & Sindo Kou

To cite this article: Chunzhi Xia & Sindo Kou (2020): Evaluating susceptibility of carbon steels to solidification cracking by transverse-motion weldability test, Science and Technology of Welding and Joining, DOI: 10.1080/13621718.2020.1812211

To link to this article: <a href="https://doi.org/10.1080/13621718.2020.1812211">https://doi.org/10.1080/13621718.2020.1812211</a>







#### RESEARCH ARTICLE



## Evaluating susceptibility of carbon steels to solidification cracking by transverse-motion weldability test

Chunzhi Xia<sup>a</sup> and Sindo Kou<sup>b</sup>

<sup>a</sup>Department of Materials Science and Engineering, Jiangsu University of Science and Technology, Zhenjiang, China; <sup>b</sup>Department of Materials Science and Engineering, The University of Wisconsin, Madison, WI, USA

#### **ABSTRACT**

The transverse-motion weldability (TMW) test was applied to carbon steels, by moving the lower sheet during lap welding at a constant speed V in the transverse direction to induce solidification cracking. A transition range of V (between no cracking at lower V and full cracking at higher V) that occurred at a lower V level indicated a higher susceptibility. The variation in the susceptibility with the carbon content of the steel was related to the Fe–C phase diagram and compared to those shown previously by other tests. The nominal critical strain rate based on the transition range was compared to the critical strain rate based on measurement by in situ observation during welding.

#### **ARTICLE HISTORY**

Received 25 June 2020 Revised 4 August 2020 Accepted 15 August 2020

#### KEYWORDS

Solidification cracking; carbon steels; welding; weldability test; transverse-motion weldability test; TMW test

#### **Nomenclature**

04C	carbon steel with 0.044 wt-% C
09C	carbon steel with 0.09 wt-% C
16C	carbon steel with 0.16 wt-% C
44C	carbon steel with 0.44 wt-% C
50C	carbon steel with 0.50 wt-% C
65C	carbon steel with 0.65 wt-% C
$\varepsilon_i$	critical strain in MISO
$\ell_0$	lateral (horizontal) distance between
	reference points at time 0 in MISO
$\ell_1$	final lateral (horizontal) distance between
	reference points at time $t_1$ in MISO
MISO	measurement by in situ observation
$t_1$	time for crack initiation
TMW test	transverse-motion weldability test
V	lower-sheet speed
W	horizontal width of weld top surface

#### Introduction

Solidification cracking is intergranular cracking that occurs in the mushy zone during welding under tension induced by solidification shrinkage and thermal contraction [1]. The transverse-motion weldability (TMW) test developed recently by Soysal and Kou [2] is illustrated in Figure 1. The lower sheet is moved slowly at a constant speed V to induce tension in the mushy zone and hence solidification cracking. The TMW test has been applied to assess the solidification cracking susceptibility of Al alloys [2–5], Mg alloys [6], stainless steels [7] and Ni-base alloys [8] but not yet to steels. Unlike the widely used Varestraint test [9], the TMW

test can induce solidification cracking by applying tension very slowly and a filler metal can be used during welding to evaluate its effect on solidification cracking. Results of the TMW test [2–8] have shown good agreement with the results based on other tests and with filler metal guides.

#### **Experimental procedure**

As shown in Table 1, six carbon steels were used in the present study, all 3.2 mm in thickness and low in S and P. Unfortunately, no such steels between 0.09 and 0.16 wt- % C, in small quantities, could be found by the authors in the US or China.

The upper sheet was 25.4 mm by 127 mm by 3.2 mm, and the lower sheet 76.2 mm by 76.2 mm by 3.2 mm. Gas tungsten arc welding (GTAW) was used as follows: welding current 110A (DCEN), arc voltage 10-11 V, torch travel speed 1.27 mm s<sup>-1</sup> and Ar gas shielding  $3.15 \times 10^{-4} \text{ m}^3 \text{ s}^{-1}$  (40 ft<sup>3</sup> h<sup>-1</sup>). The upper sheet was stationary, and the lower sheet was moved by a programmable servomotor at speed V, initially at  $0.5 \,\mathrm{mm}\,\mathrm{s}^{-1}$  to initiate crack and then lowered to a predetermined level for crack propagation. For a given steel, e.g. the 04C steel (0.044 wt-% C), the initial speed was dropped from 0.5 mm s<sup>-1</sup> to a much lower speed, e.g.  $0.10\,\mathrm{mm\,s^{-1}}$ . Since the crack did not propagate at all at 0.10 mm s<sup>-1</sup>, a significantly higher speed than  $0.10 \, \mathrm{mm \, s^{-1}}$  was then tried, e.g.  $0.25 \, \mathrm{mm \, s^{-1}}$ , and the crack propagated all the way to the weld end, i.e. full cracking. Then, a lower speed than 0.25 mm s<sup>-1</sup> was then tried. This procedure was repeated until the transition range was located.

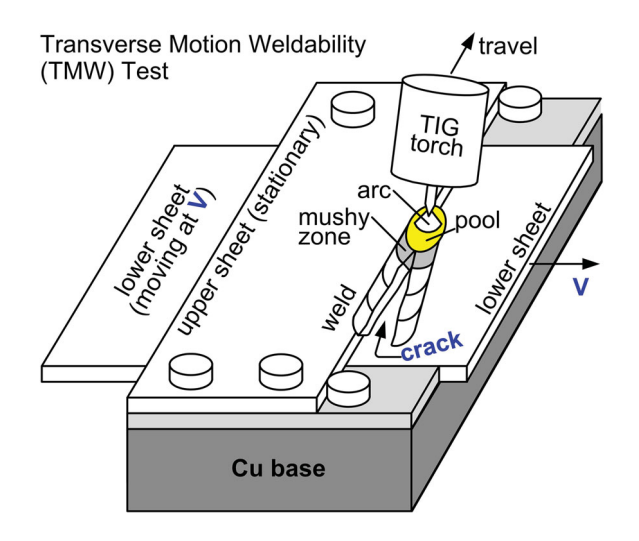


Figure 1. TMW test [2]. The lower sheet is moved in the transverse direction of welding to induce solidification cracking.

**Table 1.** Chemical compositions of the carbon steels in wt-%.

Carbon steels	C	Mn	Si	Р	S	Fe
04C	0.044	0.20	0.02	0.004	0.002	Balance
09C	0.09	0.29	0.02	0.023	0.009	Balance
16C	0.16	0.77	0.01	0.010	0.007	Balance
44C	0.44	0.89	0.21	0.014	0.0001	Balance
50C	0.50	0.69	0.24	0.010	0.003	Balance
65C	0.65	1.04	0.23	0.015	0.001	Balance

#### **Results and discussion**

#### **Crack susceptibility**

Figure 2(a) is the overview of 65C steel (0.65 wt-% C) after the TMW test at  $V = 0.05 \,\mathrm{mm/s}$ . The weld is enlarged in Figure 2(b). The normalised crack

length is defined as  $L_{\text{crack}}/L_{\text{weld}}$ , where  $L_{\text{crack}}$  is the crack length and  $L_{\text{weld}}$  the weld length corresponding to V [2–4], which is  $0.05 \,\mathrm{mm}\,\mathrm{s}^{-1}$  in this case.  $L_{\rm crack}/L_{\rm weld}~<~1~{\rm at}~V=0.05~{\rm mm\,s^{-1}}.~L_{\rm crack}/L_{\rm weld}=1$ at  $V = 0.07 \,\mathrm{mm}\,\mathrm{s}^{-1}$  as shown in Figure 2(c). In both cases, the initial speed is  $0.5 \text{ mm s}^{-1}$ .

The results of the TMW test are shown in Figure 3 by plotting the normalised crack length vs. V. The transition range indicates the range of V over which  $L_{\rm crack}/L_{\rm weld}$  rises from 0 (no crack) to 1.0 (full crack). These results will be compared with reported results based on other tests as follows.

Figure 4(a) shows the Fe-C phase diagram. The equilibrium freezing temperature range, i.e. from the liquidus temperature to the solidus temperature of the Fe-C phase diagram, is shown in Figure 4(b). Since carbon is an interstitial solute in iron, complete diffusion of C in solid and liquid, i.e. equilibrium solidification, can be assumed as an approximation. As shown, the equilibrium freezing temperature range increases with increasing C content from pure Fe to the maximum C solubility of  $\delta$ -ferrite at 0.093 wt-% C. It then decreases with increasing C content from 0.093 wt-% C to the peritectic composition of 0.172 wt-% C. Beyond the peritectic point, it increases again with further increase in the C content.

In Figure 4(c), the results of Shankar and Devletian [10] by both the Varestraint test and the transverse Varestraint test [11] show a clear peak crack susceptibility near 0.10 wt-% C. In butt welding, Ohshita et al. [12] observed a critical C content, slightly below which solidification cracking occurred and slightly

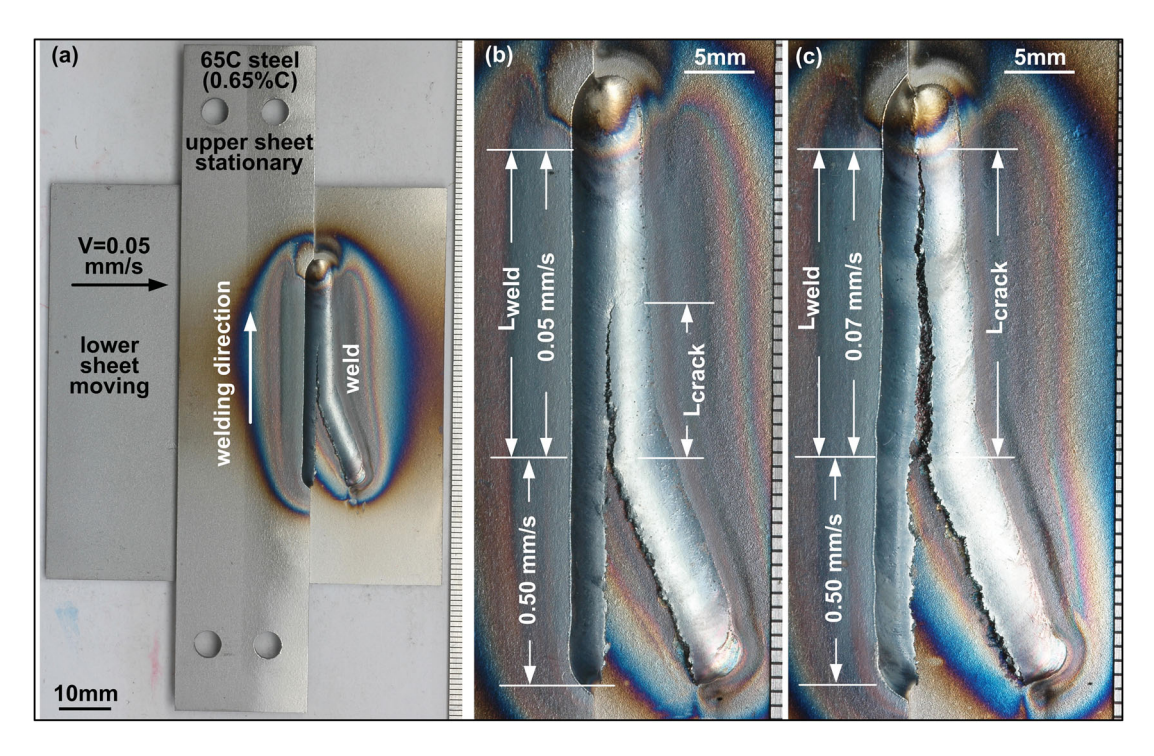


Figure 2. 65C steel (0.65 wt-% C) after TMW test: (a) overview at V = 0.05 mm s<sup>-1</sup>; (b) close-up view showing a partial crack at V = 0.05 mm s<sup>-1</sup>; (c) close-up view showing a full crack at V = 0.07 mm s<sup>-1</sup>. Lower-sheet speed V initially at 0.50 mm s<sup>-1</sup>.

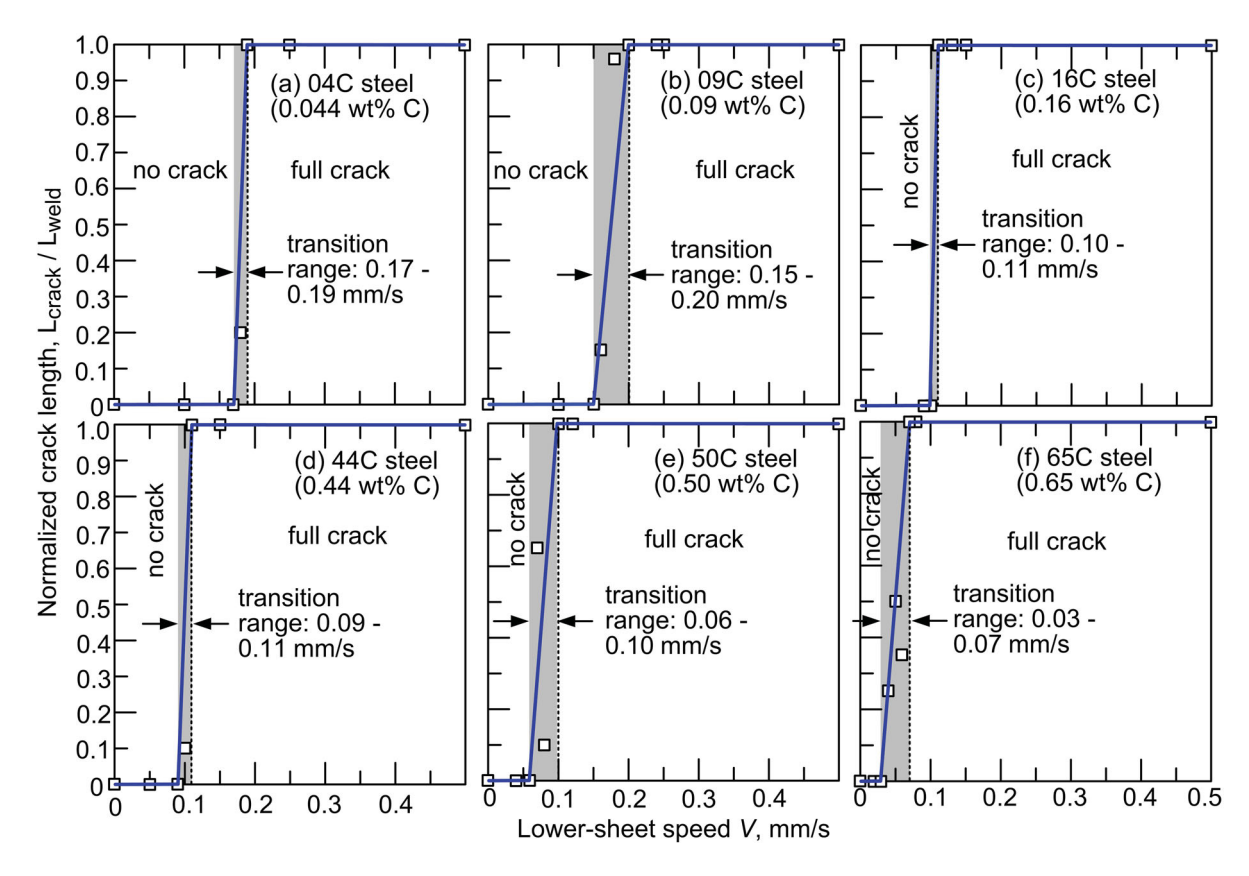


Figure 3. Results of TMW test: (a) 04C steel; (b) 09C steel; (c) 16C steel; (d) 44Csteel; (e) 50C steel; (f) 65C steel. The shaded area indicates transition from no crack to full crack.

above which solidification cracking disappeared. The critical content existed between 0.08 and 0.12 wt-% C, slightly beyond which the crack susceptibility dropped significantly.

Figure 4(d) shows the results of the TMW tests in Figure 3 by plotting the transition range in V vs. the carbon content, with V increasing downward instead of upward. The length of each vertical error bar corresponds to a transition range in Figure 3. Since the carbon steel with 0.10 wt-% C was unavailable, the peak crack susceptibility shown by the dotted line near 0.10 wt-% C is speculated in the light of the Varestraint test results in Figure 4(c) and the results of Ohshita et al. [12] mentioned previously. Other than the peak, Figure 4(d) is similar to Figure 4(c). Thus, based on Figure 4(b-d), a peak crack susceptibility exists at the maximum C solubility of 0.093 wt-% C in  $\delta$ ferrite and a minimum crack susceptibility exists at the peritectic composition of 0.172 wt-% C. Between 0.093 and 0.172 wt-% C, the equilibrium solidification range decreases with increasing C content (Figure 4b), and this explains why the crack susceptibility decreases with increasing C content in this range.

As will be shown subsequently (in Figure 5(a)), the critical strain rate to cause solidification cracking is about  $5.4\% \, \text{s}^{-1}$  at  $0.093 \, \text{wt}$ -% C and  $4.9\% \, \text{s}^{-1}$  at  $0.172 \, \text{wt}$ -% C. Ohshita et al. [12] pointed out the lateral shrinkage associated with the transformation from

 $\delta$ -ferrite to austenite  $\gamma$  is 0.0011. In the present study, thermodynamic calculation of equilibrium solidification was conducted using Pandat [13] and PanIron [14] of CompuTherm. It showed 100%  $\delta$ -ferrite forms at 0.093 wt-% C and 81.6%  $\delta$ -ferrite plus 18.4% austenite  $\gamma$  form at the peritectic composition of 0.172 wt-% C. Thus, 18.4% of 0.0011 is even smaller than 0.0011. As for the thermal expansion coefficient (CTE), as a rough approximation was made in the present study based on the study of Strycker et al. [15] on 235 steel and 304 stainless steel. It was assumed to be on the order of  $10 \times 10^{-6}$ /°C for  $\delta$ -ferrite and  $20 \times 10^{-6}$ /°C for austenite  $\gamma$ . The equilibrium freezing temperature range is about 35°C at 0.093 wt-% C and 30°C at 0.172 wt-% C (Figure 4(b)). Thus, the shrinkage caused by the CTE is  $3.5 \times 10^{-4}$  for 100%  $\delta$ -ferrite and  $6.0 \times 10^{-4}$  for 100% austenite  $\gamma$ , which is again very small. Ohshita et al. [12] attributed the susceptibility decrease beyond their critical C content of 0.08-0.12 wt-% C to the formation of austenite  $\gamma$ , which decreases the amount of  $\delta$ -ferrite that can transform to austenite  $\gamma$  to cause shrinkage and hence induce tension. However, the shrinkage caused either by  $\delta$ -to- $\gamma$  transformation or the CTE is too small to explain the significant susceptibility decrease from 0.093 to 0.172 wt-% C, which corresponds to a decrease in the critical strain rate from 5.4% s<sup>-1</sup> at 0.093 wt-% C to  $4.9\% \,\mathrm{s}^{-1}$  at  $0.172 \,\mathrm{wt}$ -% C.

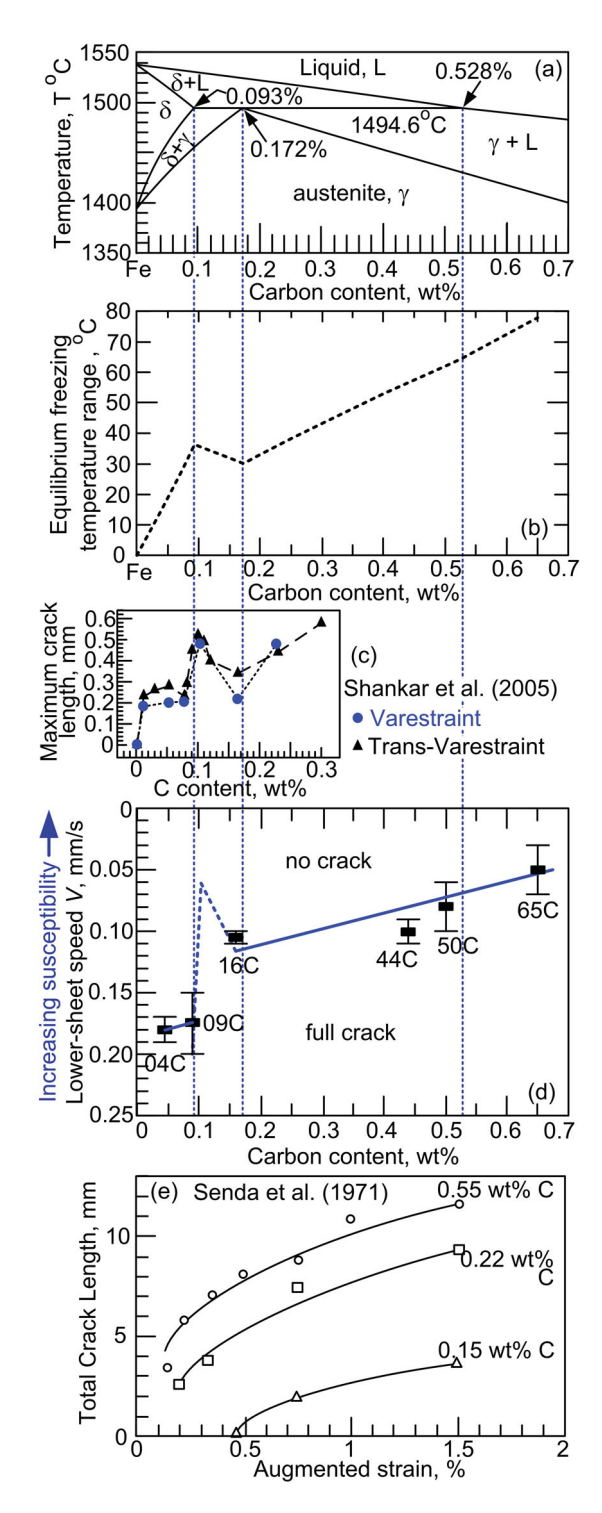


**Figure 4.** Crack susceptibility of carbon steels: (a) Fe–C phase diagram; (b) equilibrium freezing temperature range; (c) Varestraint test by Shankar and Devletian [10]; (d) TMW test (Figure 3); (e) Varestraint test by Senda et al. [11].

Figure 4(b) shows that beyond the peritectic point is at 0.172 wt-% C, the equilibrium freezing temperature range increases with increasing C content. Both the Varestraint test in Figure 4(c) and the TMW test in Figure 4(d) show, beyond the peritectic point, the susceptibility increases with increasing C content. Amaya et al. [16] used intermittent butt welding to test the solidification cracking susceptibility of carbon steels in the range of 0.13–0.25 wt-% C. Cracking did not

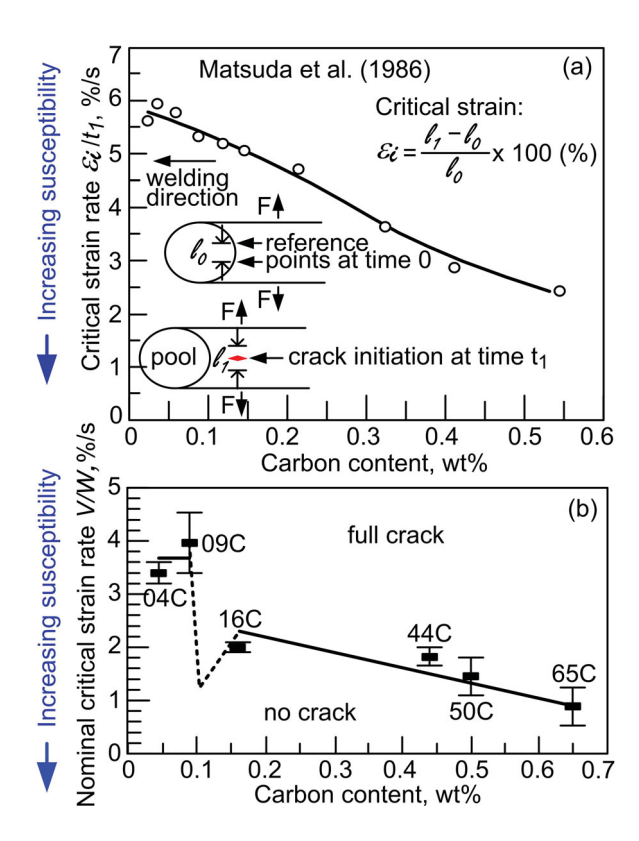


**Figure 5.** Critical strain rate: (a) tensile hot cracking test by Matsuda et al. [18]; (b) TMW test (Figure 4c).

occur below about 0.18 wt-% C but suddenly increased beyond it. This critical C content is close to the peritectic composition of 0.172 wt-% C. Using the Varestraint test, Senda et al. [11] showed in Figure 4(d) that crack susceptibility of carbon steels increases from 0.15 wt-% C (which is near 0.172 wt-% C) to 0.22 and to 0.55 wt-% C. Thus, all these four tests indicate that, beyond the peritectic point at 0.172 wt-% C, the crack susceptibility increases with increasing C content.

The phase diagram in Figure 4(a) shows beyond 0.528 wt-% C the primary solidification phase changes from  $\delta$ -ferrite to austenite  $\gamma$ . In austenitic stainless steels, primary- $\gamma$  solidification is known to be much more susceptible to solidification cracking than primary- $\delta$  solidification [1]. This can also be true for carbon steels. Furthermore, beyond 0.528 wt-% C, increasing the carbon content increases the freezing temperature range significantly and hence the crack susceptibility. The TMW test in Figure 3(d) shows 65C steel is more crack susceptible than 50C steel.

Thus, the crack susceptibility results in Figure 4 based on the TMW test and Varestraint test seem to correlate with the C content and can be explained based on the phase diagram. This may suggest that carbon plays a dominant role in the solidification cracking of these steels, but other elements need to be considered as well. As shown in Table 1, elements other than C were also present in these steels, such as Mn, Si, P and S. S and P are known to increase the crack susceptibility of steels. They affect the crack susceptibility more

significantly than Mn and Si. The S content is very low (0.001-0.003 wt-%) except for steels 09C and 16C. Steel 09C contained 0.009 wt-% S and 0.29 wt-% Mn, and the Mn/S ratio was 32.2. Steel 16C contained 0.007 wt-% S and 0.77 wt-% Mn, and the Mn/S ratio was 110. Smith [17] showed no solidification cracking in carbon steels at 0.09 wt-% C if Mn/S > 9 and no cracking at 0.16 wt-% C if Mn/S > 55. Thus, S in steels 09C and 16C might not have a significant effect on their crack susceptibility. The P content was about constant at 0.012 wt-% except for steel 04C (0.004 wt-% P) and steel 09C (0.023 wt-% P). Steel 09C had twice more P than steel 16C (0.010 wt-% P) but a lower crack susceptibility than steel 16C. Thus, the higher P content (0.023 wt-%) of steel 09C could not have increased its crack susceptibility significantly. The calculation of the susceptibility of Fe-C alloys as a function of the C content will be published elsewhere.

#### Critical strain rate

Matsuda et al. [18] used the technique of measurement by in situ observation (MISO) to study solidification cracking. In their tensile hot cracking test, the workpiece was mounted on a horizontal tensile testing machine and stretched in the transverse direction of bead-on-plate welding. As illustrated in Figure 5(a), the lateral distance between two reference points at the pool boundary  $\ell_0$  at time 0 are recorded. When the lateral distance increases to  $\ell_1$ , cracks are initiated between these points at time  $t_1$ . The critical strain is taken as  $\varepsilon_i = \left[ (\ell_1 - \ell_0) / (\ell_0) \right] \times 100\%$  and the critical strain rate as  $\epsilon_i / t_1$ . As shown, as the carbon content increases from about 0.025 to 0.55 wt-% C, the critical strain rate decreases smoothly, that is, the crack susceptibility increases smoothly.

As shown in Figure 5(b), the lower-sheet speed *V* in Figure 4(c) is divided by the horizontal width of the weld top surface W. An example is  $W = 6.4 \,\mathrm{mm}$  for the 44C steel tested at  $V = 0.11 \text{ mm s}^{-1}$ . Table 2 shows the value of W taken from the upper end of the transition range of each steel, e.g. at  $V = 0.11 \,\mathrm{mm}\,\mathrm{s}^{-1}$  for 44C steel. During the time interval dt, the weld edge on the top surface of the lower sheet moves horizontally by Vdt. This causes a nominal strain of Vdt/W and hence a nominal strain rate of (Vdt/W)/dt or V/Win the horizontal direction. The transition range of

**Table 2.** Nominal strain rate at weld top surface.

Carbon steels	Transition range <i>V</i> , mm s <sup>-1</sup>	Width of weld <i>W</i> , mm	Nominal strain rate <i>V/W</i> , % s <sup>-1</sup>
04C	0.17-0.19	5.3	3.20–3.58
09C	0.15-0.20	4.4	3.41-4.54
16C	0.10-0.11	5.3	1.89-2.08
44C	0.09-0.11	6.4	1.41-1.72
50C	0.06-0.10	5.6	1.07-1.79
65C	0.03-0.07	5.7	0.53-1.23

*V/W* from no cracking to full cracking can be taken as the nominal critical strain rate at the weld top surface in the horizontal direction. When compared with the critical strain rate shown in Figure 5(a), which is in the horizontal direction, the transition range of V/Whas the same order of magnitude and it also decreases with increasing carbon content. However, a sudden drop is likely to exist near 0.10 wt-% C, corresponding to the peak crack susceptibility near 0.10 wt-% C in Figure 4(c).

#### **Conclusions**

- (1) The TMW test can be applied to carbon steels to evaluate their susceptibility to solidification cracking. The transition range in the lower-sheet speed V (from no cracking to full cracking) can be used as the index for the crack susceptibility - the lower the V level of the transition range is, the higher the crack susceptibility.
- (2) The relative crack susceptibility of the six carbon steels evaluated by the TMW test is consistent with that reported previously based on other tests.
- (3) The nominal critical strain rate based on the range of V/W has the same order of magnitude as the critical strain rate of Matsuda et al. [18].

#### **Acknowledgements**

C.X. was supported by the Jiangsu Overseas Visiting Scholar Program for University Prominent Young & Middle-aged Teachers and Presidents as a visiting professor at the University of Wisconsin-Madison from 2018 to 2019. S.K. was supported by the National Science Foundation initially under Grant Number DMR 1500367 and subsequently under Grant Number DMR1904503.

#### Disclosure statement

No potential conflict of interest was reported by the author(s).

#### **Funding**

C.X. was supported by the Jiangsu Overseas Visiting Scholar Program for University Prominent Young & Middle-aged Teachers and Presidents as a visiting professor at the University of Wisconsin-Madison from 2018 to 2019. S.K. was supported by the National Science Foundation initially under Grant Number DMR 1500367 and subsequently under Grant Number DMR1904503.

#### References

- [1] Kou S. Welding metallurgy. 3rd ed. Hoboken (NJ): John Wiley and Sons; 2020.
- [2] Soysal T, Kou S. A simple test for solidification cracking susceptibility and filler metal effect. Weld J. 2017;96(10):389s-401s.
- [3] Soysal T, Kou S. Effect of filler metals on solidification cracking susceptibility of Al Alloys 2024 and 6061. J Mater Proc Tech. 2019;266:421-428.

- [4] Soysal T, Kou S. A simple test for assessing solidification cracking susceptibility and checking validity of susceptibility prediction. Acta Mater. 2018;143:181–197.
- [5] Soysal T, Kou S. Role of liquid backfilling in reducing solidification cracking in aluminum welds. Sci Technol Weld Joining. 2020;25(5):415–421.
- [6] Liu K, Kou S. Susceptibility of magnesium alloys to solidification cracking. Sci Technol Weld Joining. 2020;25(3):251–257.
- [7] Liu K, Kou S. Susceptibility of stainless steels to solidification cracking: new test and explanation. Weld J. 2020;99(October):1s.
- [8] Xia C, Kou S. Evaluating susceptibility of Ni-base alloys to solidification cracking by transverse-motion weldability test. Sci Technol Weld Joining. 2020: 13). https://doi.org/10.1080/13621718.2020.1802897.
- [9] Savage WF, Lundin CD. The varestraint test. Weld J. 1965;44(10):433s-442s.
- [10] Shankar V, Devletian JH. Solidification cracking in low alloy steel welds. Sci Technol Weld Joining. 2005;10(2):236–243.
- [11] Senda T, Matsuda F, Takano G, et al. Fundamental investigations on solidification crack susceptibility for weld metals with trans-varestraint test. Trans Jpn Weld Soc. 1971;2(2):141–162.

- [12] Ohshita S, Yurioka N, Mori N, et al. Prevention of solidification cracking in very low carbon steel welds. Weld J. 1983;62(5):129s-136s.
- [13] Pandat. Phase diagram calculation software package for multicomponent systems. Madison (WI): Computherm LLC; 2019.
- [14] PanIron. Thermodynamic database for commercial iron alloys. Madison (WI): Computherm LLC; 2019.
- [15] Strycker MD, Schueremans L, Paepegem WV, et al. Measuring the thermal expansion coefficient of tubular steel specimens with digital image correlation techniques. Opt Laser Eng. 2010;48(10):978–986.
- [16] Amaya T, Yonezawa T, Ogawa K, et al. Solidification cracking mechanism of carbon steel weld metal. Weld J. 2018;97(2):55s–64s.
- [17] Smith RB. Arc welding of carbon steels. In: Olson DL, Siewert TA, Liu S, et al., editors. ASM handbook. Vol.6 welding, brazing and soldering. Materials Park (OH): ASM International; 1993. p. 641–661.
- [18] Matsuda F, Nakagawa H, Tomita S. Quantitative evaluation of solidification brittleness of weld metal during solidification by in-situ observation and measurement (Report III). Trans JWRI. 1986;15(2): 297–305.